applied biosciences

MDPI

Article

Computational Approach to Possible Interactions of Gliclazide with Proteins of Inflammatory, Oxidative Stress and Endoplasmic Reticulum Stress Pathways

Olabisi Tajudeen Obafemi [1,*], Ademola Olabode Ayeleso [1,2], Blessing Ariyo Obafemi [3], Jeremiah Oshiomame Unuofin [1], Adewale Odunayo Oladipo [1], Sogolo Lucky Lebelo [1] and Monde Ntwasa [1]

[1] Department of Life and Consumer Sciences, University of South Africa, Johannesburg 1709, South Africa; ademola.ayeleso@bowen.edu.ng (A.O.A.); unuofinjeremiah@gmail.com (J.O.U.); walexy20002001@gmail.com (A.O.O.); lebelol@unisa.ac.za (S.L.L.); ntwasmm@unisa.ac.za (M.N.)
[2] Biochemistry Programme, College of Agriculture, Engineering and Sciences, Bowen University, Iwo PMB 284, Osun State, Nigeria
[3] Department of Medical Biochemistry, Afe Babalola University, Ado-Ekiti PMB 5454, Ekiti State, Nigeria; blessingafolabi7@gmail.com
* Correspondence: oobafemi@abuad.edu.ng; Tel.: +27-638695069

Abstract

The present study aims to evaluate the interaction of gliclazide with proteins related to inflammation—{inhibitor of nuclear factor kappa-B kinase subunit beta (IKKα) and NF-kappa-B-inducing kinase (NIK)}; oxidative stress—{kelch domain of Kelch-like ECH-associated protein 1 (KKeap1)} and ER stress—{inositol-requiring enzyme-1alpha (IRE1α)}. X-ray crystal structure of IKKα, (PDB ID: 5EBZ), KKeap1 (PDB ID: 4L7B), NIK (PDB ID: 8YHW) and IRE1α (PDB ID: 4YZ9) were obtained from Protein Data Bank and Open Babel 3.1.1 was used to prepare the ligands. Prior to docking, protein structures were prepared by removing water molecules, adding hydrogen atoms, and optimizing side chain conformations using Maestro (Schrödinger Suite, version 2024-2) along with the OPLS4 force field. Ligand docking was performed using the Glide application. Molecular dynamics simulation was performed with Desmond (Schrödinger Suite) within the Maestro interface for 100 ns for the NPT ensemble at 300 K and 1 atm pressure. Physicochemical and pharmacokinetics properties were analyzed using ADMETlab 3.0 and SwissADME. The binding energies of gliclazide with IKKα, NIK, KKeap1 and IRE1α were −8.3, −7.9, −8.4 and −8.8, respectively. Root mean square displacement (RMSD), root mean square fluctuation (RMSF) and radius of gyration analyses predicted relatively strong and stable interactions between gliclazide and the proteins, with favourable pharmacokinetic properties. It was also observed that CYP3A4 metabolizes gliclazide, in addition to CYP2C9 and CYP2C19. The activity of gliclazide against inflammation, oxidative stress and endoplasmic reticulum stress might be via interaction with these proteins.

Keywords: gliclazide; inflammation; ER stress; docking; diabetes mellitus

Check for updates

Received: 25 September 2025
Revised: 28 November 2025
Accepted: 5 January 2026
Published: 14 February 2026

Copyright: © 2026 by the authors. Licensee MDPI, Basel, Switzerland. This article is an open access article distributed under the terms and conditions of the Creative Commons Attribution (CC BY) license.

1. Introduction

Diabetes mellitus is a serious and long-term disease arising from either the inability of the pancreas to produce adequate insulin or the inability of the body to effectively utilize the insulin produced by the pancreas. Hyperglycemia, a common indicator of uncontrolled diabetes, may eventually lead to various diabetic complications affecting the eyes, blood vessels, nerves, heart and kidneys [1]. In 2017, diabetes was responsible for about 3% of

global mortality and ranked among the first ten causes of adult deaths, with about US$ 727 billion expended on the disease [2,3]. There are three main types of diabetes, namely type 1 diabetes (T1DM), type 2 diabetes mellitus (T2DM) and gestational diabetes (GDM); however, type 2 diabetes accounts for about 90% of all cases. In 2019, the prevalence rate of diabetes was estimated to be 9.3%, translating to about 463 million people, and these figures are projected to rise to 10.2% (578 million people) by 2030 and 10.9% (700 million people) by 2045 [4].

Previous studies have confirmed the involvement of oxidative stress, inflammation and endoplasmic reticulum (ER) stress in diabetes [5,6]. Oxidative stress has been implicated in derangement of insulin synthesis, secretion and action, which are all important features of type 2 diabetes. Persistent hyperglycemia, which is a major characteristic of type 2 diabetes, precipitates inflammation, oxidative stress, amyloid stress, accumulation of misfolded insulin, and eventually, endoplasmic reticulum (ER) stress, especially in the β-cells, because of their genetic susceptibility [7]. Moreover, glucotoxicity, lipotoxicity and glucolipotoxicity, which occur in obesity and type 2 diabetes, instigate oxidative stress that eventually damages the β-cells [8]. Moreover, the oxidative stress associated with diabetes contributes to the development and progression of complications of diabetes [9]. The ability of any one of the following—oxidative stress, inflammation, or endoplasmic reticulum stress—to potentiate the other two in the settings of type 2 diabetes has been previously reported [6,10,11].

Gliclazide is an oral antidiabetic drug (OAD) belonging to the class of sulfonylureas, which has been identified as the second most prescribed class of OADs. However, gliclazide stands out among other sulfonylureas, not only because it is associated with significantly lower incidences of hypoglycemia but also because it provides significant antioxidant benefits, which potentially reduces the likelihood of developing diabetic complications. Moreover, based on its effectiveness and patient status, gliclazide has been recommended as a first- or second-line antidiabetic agent for managing T2DM [9,12]. In addition to metformin, gliclazide is the only oral antidiabetic drug on the WHO essential medicines list [13]. While both metformin and gliclazide were reported to have antioxidant effects, it was reported that gliclazide possesses better antioxidant effects than metformin [14], an effect that might not be unconnected with the azabicylooctyl ring in its structure [15].

In the presence of various pro-inflammatory stimuli, the nuclear factor kappa-light-chain-enhancer of activated B cells (NF-κB) is quickly activated by the IκB kinase (IKK) complex and released from its binding to the inhibitor of NF-κB (IκB). The IKK complex consists of three subunits, two of which are catalytic (IKKα and IKKβ), while the third subunit (IKKγ/NEMO) has a regulatory function. IKK activation results in IκB phosphorylation and ubiquitination. As a result, free NF-κB can translocate into the nucleus and influence the expression of several target genes [16]. NF-kB-inducing kinase (NIK) is an important upstream modulator of the alternative NF-kB signalling pathway [17]. In non-stimulated cells, NIK is usually tethered to both tumour necrosis factor receptor-associated factor 2 and 3 (TRAF2/3) and cellular inhibitor of apoptosis protein 1 and 2 (cIAP1/2), thereby causing its ubiquitination and constant degradation. Upon stimulation with cytokines and other stimuli, NIK unbinds from TRAF2/3, which is degraded, thereby allowing NIK to accumulate, stabilize, and subsequently activate the non-canonical NF-kB pathway [18]. Previous studies have implicated NIK in insulin resistance based on its induction in the liver of obese mice and muscle of obese humans and in T2D-associated β-cell failure [19].

IKKα is a regulator of the non-canonical NF-κB activation pathway as it is involved in the phosphorylation of p100, thereby facilitating the processing of p100 to p52. p52 then forms a heterodimer with RelB (p52:RelB) [20], which then translocates to the nucleus where it activates NF-κB target genes in lymphoid cells that are implicated in develop-

mental programmes [21]. It was previously suggested that IKKα contributes to canonical activation of the NF-κB pathway. More recent studies have shown that IKKα might be the principal kinase of the NF-κB pathway as it adequately compensated for IKKβ activity in IKKβ-knockout cells while IKKβ did not compensate for IKKα activity in IKKα-knockout cells [22,23]. A previous study reported that both interleukin-1β and tumour necrosis factor-α are able to activate the non-canonical NF-κB pathway in beta cells, suggesting a role for IKKα in pancreatic inflammatory process [24]. Moreover, IKKα has been reported to regulate IKKβ activity via phosphorylation, thereby making IKKα a potential contributor to the downstream effects of IKKβ [15]. This is quite instructive as IKKβ is known to interfere directly with the insulin signalling pathway and cause insulin resistance in the liver, adipose tissue and skeletal muscles. Thus, IKKα may have modulatory effects on insulin signalling [25–27].

Usually, cells sense accumulation of misfolded proteins in the endoplasmic reticulum (ER) through three ER resident transmembrane proteins viz. inositol, requiring enzyme-1α (IRE1α), protein Kinase-R-like ER kinase (PERK), and activating transcription factor-6 (ATF6) [28,29]. These proteins become activated and then set off a series of transcription processes after dissociating from their interaction with glucose-regulated protein-78 (GRP78) in the ER lumen. The initial goal of these three ER sensors and their downstream effectors is to ultimately restore ER homeostasis through the three mechanisms stated earlier, a phenomenon known as unfolded protein response (UPR). However, failure to achieve this eventually directs the UPR to switch to a chronic ER stress whose output includes cell destruction and apoptosis, as evidenced by a decline in pancreatic beta-cell mass observed in ER stress-associated diabetes mellitus [30]. An earlier study reported that the IRE1α branch of the ER stress, which is the most evolutionarily conserved among the three ER stress sensors [31], contributes significantly to the amelioration of oxidative stress and regulation of inflammatory cytokine generation under several stress conditions [32]. Defects in the IRE1α pathway lead to deranged processing of proinsulin, diminished insulin secretion, lack of adaptive proliferation of the β-cells and β-cell death [33,34].

Kelch-like ECH-associated protein 1 (Keap1) serves as a stress sensor in the cell, and the modifications of its primary structure during oxidative or electrophilic stress leads to a disruption in its interaction with, and eventually the stabilization of Nrf2 [35,36]. Studies have shown that the dysregulation of the Nrf2/Keap1/ARE pathway is implicated in the pathophysiology of diabetes mellitus as well as its complications, and the pathway has been identified as a promising drug target for insulin resistance and sensitivity, pancreatic dysfunction and a wide range of diabetic complications [37]. It has been established that the binding of Nrf2 to Keap1 is via the kelch domain of Keap1, suggesting that the kelch domain of Keap1 plays an important role in the regulation of the Nrf2/Keap1/ARE pathway [38].

Gliclazide has recently been receiving significant consideration due to its antioxidant and anti-inflammatory properties, in vitro and in vivo [39]. The aminoazabicyclo-octane ring of gliclazide was reported to protect the beta-cells against oxidative stress, thereby contributing to reduced beta-cell death and reduced treatment failure in gliclazide use [40]. This study, therefore, aimed to use an in silico model to evaluate the interaction of gliclazide with proteins associated with ER stress (IRE1α), oxidative stress (KKeap1) and inflammation (IKKα and NIK), which are critical pathways involved in the pathogenesis and progression of diabetes mellitus, as well as to highlight some of its pharmacokinetic properties.

2. Materials and Methods

2.1. Protein Preparation

The X-ray crystal structure of inhibitor of KappaB kinase alpha (IKKα) (PDB ID: 5EBZ) [41], Kelch-domain of Kelch-like ECH-associated-protein 1 (KKeap1) (PDB

ID: 4L7B) [42], NF-kappaB-inducing kinase (NIK) (PDB ID: 8YHW) [43] and inositol-requiring enzyme-1α (IRE1α) (PDB ID: 4YZ9) [44] were obtained from Protein Data Bank (https://www.rcsb.org/ (accessed on 5 August 2025)) [45]. Co-crystalized ligands used for the proteins were 2-azanyl-5-phenyl-3-(4-sulfamoylphenyl)benzamide (5TL) for IKKα, [46], (1S,2R)-2-{[(1S)-1-[(1,3-dioxo-1,3-dihydro-2H-isoindol-2-yl)methyl]-3,4-dihydroisoquinolin-2(1H)-yl]carbonyl}cyclohexanecarboxylic acid (1VV) for KKeap1 [47], (5*R*)-2-(3,4-dichlorobenzyl)-*N*-(4-methylbenzyl)-2,7-diazaspiro(4.5)decane-7-carboxamide (4K7) Ire1α [48], and phosphothiophosphoric acid-adenylate ester for NIK [49]. All the proteins are human proteins. The proteins were prepared using Glides protein preparation wizard (Schrodinger Inc., New York, NY, USA). In the preparation steps, the water of crystallization that is not so crucial for the process was deleted to make the modelling simpler. The loops and atoms that are essential to the structures were fixed using loop refinement methods. Receptor grids were generated using Receptor grid generation in the Glide application for proteins having co-crystalized ligands.

2.2. Ligand Preparation

Ligand preparation was performed with the involvement of energy minimization and generation of rotatable bonds using Open Babel (OpenEye Scientific, Santa Fe, NM, USA).

2.3. Molecular Docking Modelling

The molecular docking was specifically executed utilizing Maestro (Schrödinger Suite, version 2024-2) along with the OPLS4 force field (Schrodinger Inc., New York, NY, USA), in a quest to investigate the binding interactions between gliclazide and the target protein structures. During the preparation steps, water molecules situated more than 5.0 Å from the binding site were eliminated to make the modelling process easier. These molecules do not have any direct role in the binding of ligands. On the other hand, water molecules that are structurally conserved and located within 3.0 Å of both the protein binding site and co-crystallized ligands were kept if they were present in the crystal structures. This is because these waters can be the ones that facilitate crucial protein–ligand interactions. The receptor was treated through the Protein Preparation Wizard, which included the process of protonation at a pH of 7.0 ± 0.5 and the implementation of restrained minimization. The ligands were produced through LigPrep (Schrodinger Inc., New York, NY, USA) with the aim of having low-energy 3D structures and the right ionization states. The grid for the binding site was created based on the co-crystallized ligand. Glide docking was performed with Standard Precision (SP) to create initial poses, then the top hits were subjected to Extra Precision (XP) redocking to achieve refined poses along with XP Glide Scores.

2.4. Molecular Dynamics Simulation

Molecular dynamics simulations were carried out with Desmond (Schrödinger Suite) within the Maestro interface for 100 ns for the NPT ensemble at 300 K and 1 atm pressure. During simulation setup, the oligomerization states of the target proteins were taken into consideration. For IKKα (PDB: 5EBZ), the structure was set up as a single monomer representing the catalytic domain, and it was simulated as such. The same approach was used for NIK (PDB: 8YHW), where the monomer of the kinase domain was considered. KKeap1 (PDB: 4L7B) has the Kelch domain, which is typically a homodimer; thus, this dimeric structure was maintained during the MD simulations by including both chains in the simulation system. IRE1α (PDB: 4YZ9) is the kinase domain monomer. The simulation boxes were sized properly to keep the interactions between the periodic images from becoming artificial and affecting the simulation. The complexes of protein and ligand were solvated within the TIP3P explicit water model with appropriate salt concentration to neutralize the system. It is important to mention that the first docking was performed

with the least number of water molecules possible, to make conformational sampling quick, while later on, the MD simulations were performed in explicit TIP3P water to test the stability and dynamics of the predicted binding poses under physiological conditions. This approach is very common in computational drug discovery, where docking finds possible binding modes, and MD simulations confirm their stability in a completely solvated environment. The merging of RMSD values and stable protein–ligand interactions for the duration of the 100 ns MD simulations is a guarantee that the initially predicted binding poses were stable under the condition of explicit solvation, thus proving our docking predictions right. Independent correlation analysis was carried out for both the ligand property and the protein–ligand interaction property to study their relationship with binding stability. Trajectory analysis included RMSD, RMSF, and the calculation of protein–ligand interaction fraction to explore complex stability and conformational dynamics throughout the simulation period.

2.5. Pharmacokinetic Parameters

Physicochemical and pharmacokinetics properties were analyzed using ADMETlab 3.0 and SwissADME.

3. Results

3.1. Molecular Docking

The docking score for binding of gliclazide and protein co-crystalized ligands to the proteins as indicated in Table 1 are IKKα [−8.3, −9.9], NIK [−7.9, −8.1], KKeap1 [−8.4, −10.6] and IRE1α [−8.8, −10.9] kcal/mol. The results show that gliclazide demonstrated appreciable binding to the proteins of interest and compared favourably with the co-crystalized ligands of respective proteins. The 2D presentations of gliclazide in the binding pockets of the proteins and their co-crystalized ligands, as well as the various amino acids that gliclazide interacts with in the binding pockets are shown in Figure 1. In the binding pockets, gliclazide was revealed to interact with a number of important amino acid residues, as depicted in Figure 1. From the IKKα α perspective (Figure 1a), the ligand formed two hydrogen bonds with Glu97 and Cys99; it also engaged Val29, Ala42, and Val74 in hydrophobic interactions. KKeap1 (Figure 1c) was the next to be considered, and the ligand bonded with Arg415, Asn382, and Ser508 through hydrogen bonding; besides that, there was pi–pi stacking with Tyr525. NIK (Figure 1e) was the next receptor considered, and it formed hydrogen bonds with Asp545 and Glu565, while also having hydrophobic contact with Leu478, Val482, and Ile538.The last one was IRE1α (Figure 1g), where gliclazide connected Lys599 and Asp711 through hydrogen bonds while hydrophobic contacts were made with Leu588, Val609, and Phe712. All these different interactions are what gave the high binding affinity of gliclazide noted for all target proteins.

Table 1. Extra Precision (XP) Score docking score of gliclazide with IKKα, KKeap1, NIK and IRE1α.

Proteins	XP Score				
	Gliclazide	**5TL**	**IVV**	**AGS**	**4K7**
IKKα	−8.3	−9.9	-	-	-
NIK	−7.9	-	-	−8.1	-
KKeap1	−8.4	-	−10.6	-	-
IRE1α	−8.8	-	-	-	−10.9

IKK-α—inhibitor of nuclear factor kappa-B kinase subunit alpha; NIK—NF-kappa-B-inducing kinase (NIK); KKeap1—Kelch-like ECH-associated protein 1; IRE1α—inositol-requiring enzyme 1-alpha. 5TL = Co-Crystalized Ligand of IKKα, IVV = Co-Crystalized Ligand of KKeap1, AGS = Co-Crystalized Ligand of NIK, 4K7 = Co-Crystalized Ligand of IRE1α.

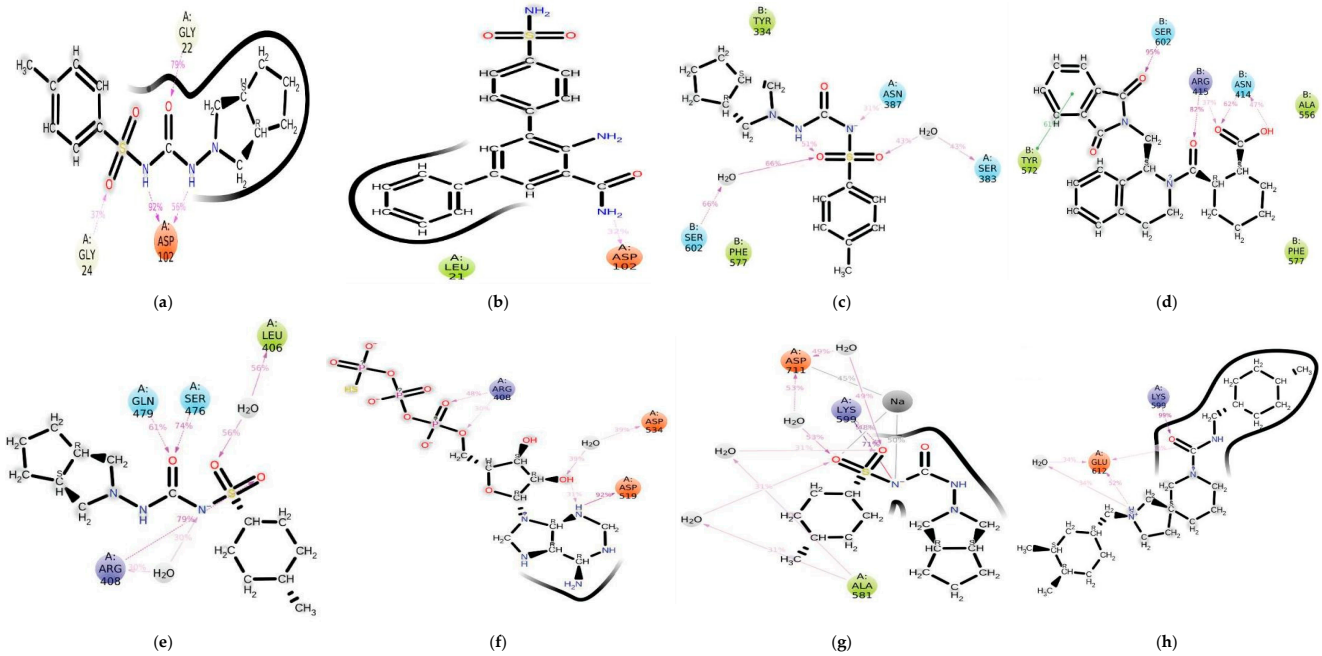


Figure 1. Post-docking analysis of binding of gliclazide and co-crystalized ligands of proteins with the proteins. (**a**) = gliclazide + IKKα, (**b**) = 5TL + IKKα, (**c**) = gliclazide + KKeap1, (**d**) = IVV + KKeap1, (**e**) = gliclazide + NIK, (**f**) = AGS + NIK, (**g**) = gliclazide + IRE1α, (**h**) = 4K7 + IRE1α. Key: IKK-α—inhibitor of nuclear factor kappa-B kinase subunit alpha; NIK—NF-kappa-B-inducing kinase (NIK); KKeap1—Kelch-like ECH-associated protein 1; IRE1α—inositol-requiring enzyme 1-alpha. 5TL—co-crystalized ligand of IKKα, IVV—co-crystalized ligand of KKeap1, AGS—co-crystalized ligand of NIK, 4K7—co-crystalized ligand of IRE1α.

3.2. Molecular Dynamic Simulation

3.2.1. Root Mean Square Deviation

The structural stability of the complexes was assessed using the root mean square deviation (RMSD) of the backbone atoms relative to the protein. This offers details on the long-term stability and convergence of protein–gliclazide complexes and protein-reference compounds complexes, as indicated in Figure 2. The average RMSD values recorded for the four-system apoprotein and protein–ligand complexes for IKKα, KKeap1, NIK and IRE1α were [4.010, 0.57063], [2.877, 0.32619], [2.489, 0.55344] and [2.265, 0.26111], respectively. This investigation of RMSD profiles between apo-proteins and protein–ligand complexes indicated that in most cases, ligand binding led to the stabilization of protein structures. The average RMSD of the apo-protein was higher (4.010 ± 0.571 Å) than that of the gliclazide-bound complex (0.571 ± 0.035 Å) for IKKα. The same stabilization patterns were noticed for KKeap1, NIK, and IRE1α, where ligand binding diminished the structural fluctuations and therefore suggested protein–ligand interactions as the reason for the stabilization.

3.2.2. Root Mean Square Fluctuation Analysis

As shown in Figure 3, the root mean square fluctuation (RMSF) average values of the four-system apoprotein and protein–ligand complexes for IKKα, KKeap1, NIK and IRE1α were [1.095, 0.34983], [0.968, 0.36919], [0.662, 0.23488] and [0.409, 0.11631], respectively. High RMSF occurred in the protein's flex regions. The most fluctuating regions of the protein were the loop portions since they were considered the most flexible. The constrained residues regions, where the ligands bind, are the other regions that had a lower degree of variability.

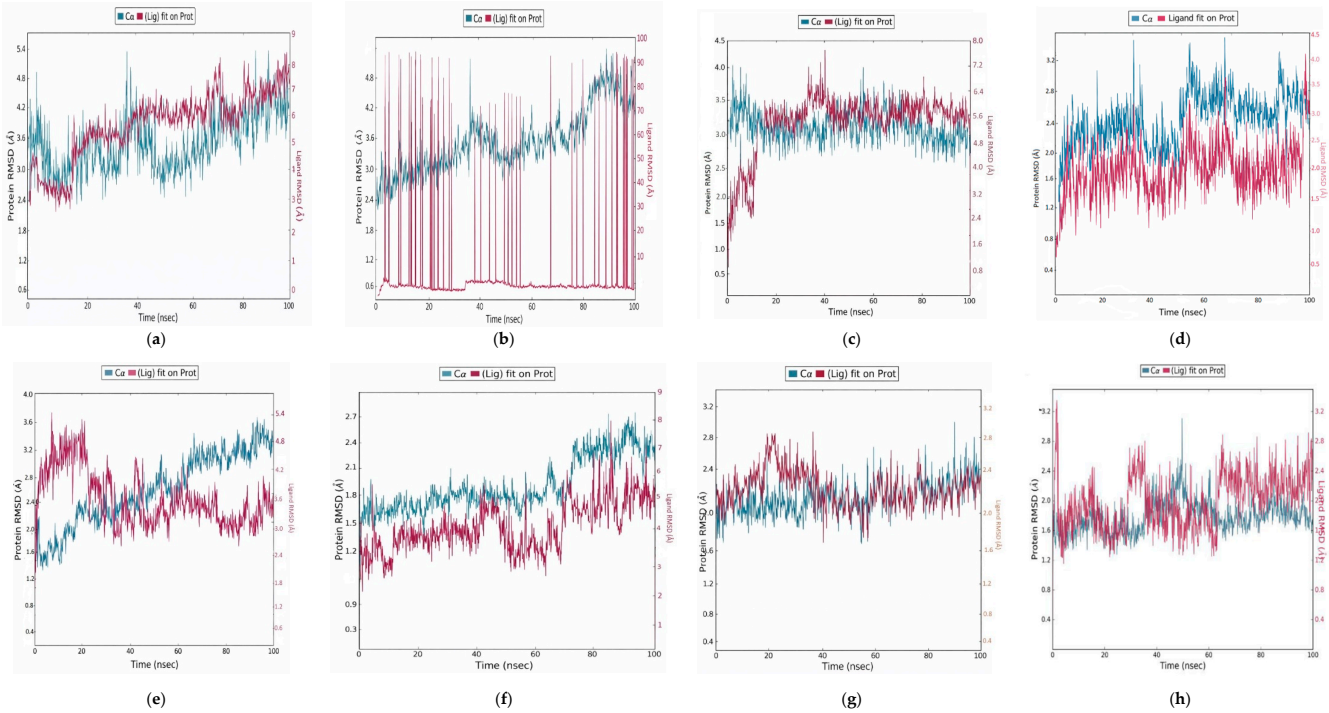


Figure 2. Root mean square deviation plot as a function of simulation time of gliclazide and co-crystalized ligands dynamics binding to IKKα, KKeap1, NIK and IRE1α. (**a**) = gliclazide + IKKα, (**b**) = 5TL + IKKα, (**c**) = gliclazide + KKeap1, (**d**) = IVV + KKeap1, (**e**) = gliclazide + NIK, (**f**) = AGS + NIK, (**g**) = gliclazide + IRE1α, (**h**) = 4K7 + IRE1α. 5TL = co-crystalized ligand of IKKα, IVV = co-crystalized ligand of KKeap1, AGS = co-crystalized ligand of NIK, 4K7 = co-crystalized ligand of IRE1α.

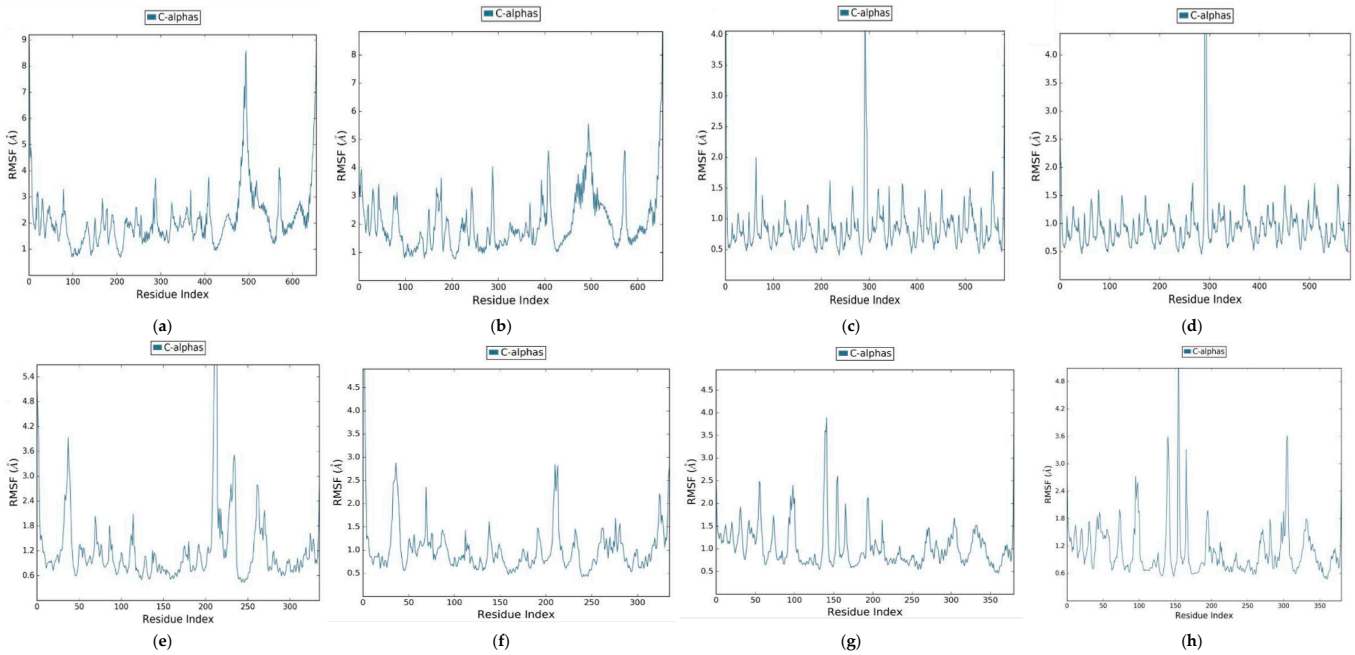


Figure 3. Root mean square fluctuation plot as a function of simulation time of gliclazide and co-crystalized ligands dynamics binding to IKKα, KKeap1, NIK and IRE1α. (**a**) = gliclazide + IKKα, (**b**) = 5TL + IKKα, (**c**) = gliclazide + KKeap1, (**d**) = IVV + KKeap1, (**e**) = gliclazide + NIK, (**f**) = AGS + NIK, (**g**) = gliclazide + IRE1α, (**h**) = 4K7 + IRE1α. 5TL = co-crystalized ligand of IKKα, IVV = co-crystalized ligand of KKeap1, AGS = co-crystalized ligand of NIK, 4K7 = co-crystalized ligand of IRE1α.

3.2.3. Radius of Gyration

The radius of gyration (Rg) values of the four-system apoprotein and protein–ligand complexes for IKKα, KKeap1, NIK and IRE1α were [2.117, 0.37407], [2.544, 0.52147], [1.436, 0.11834] and [1.025, 0.14470], respectively, as indicated in Figure 4 below.

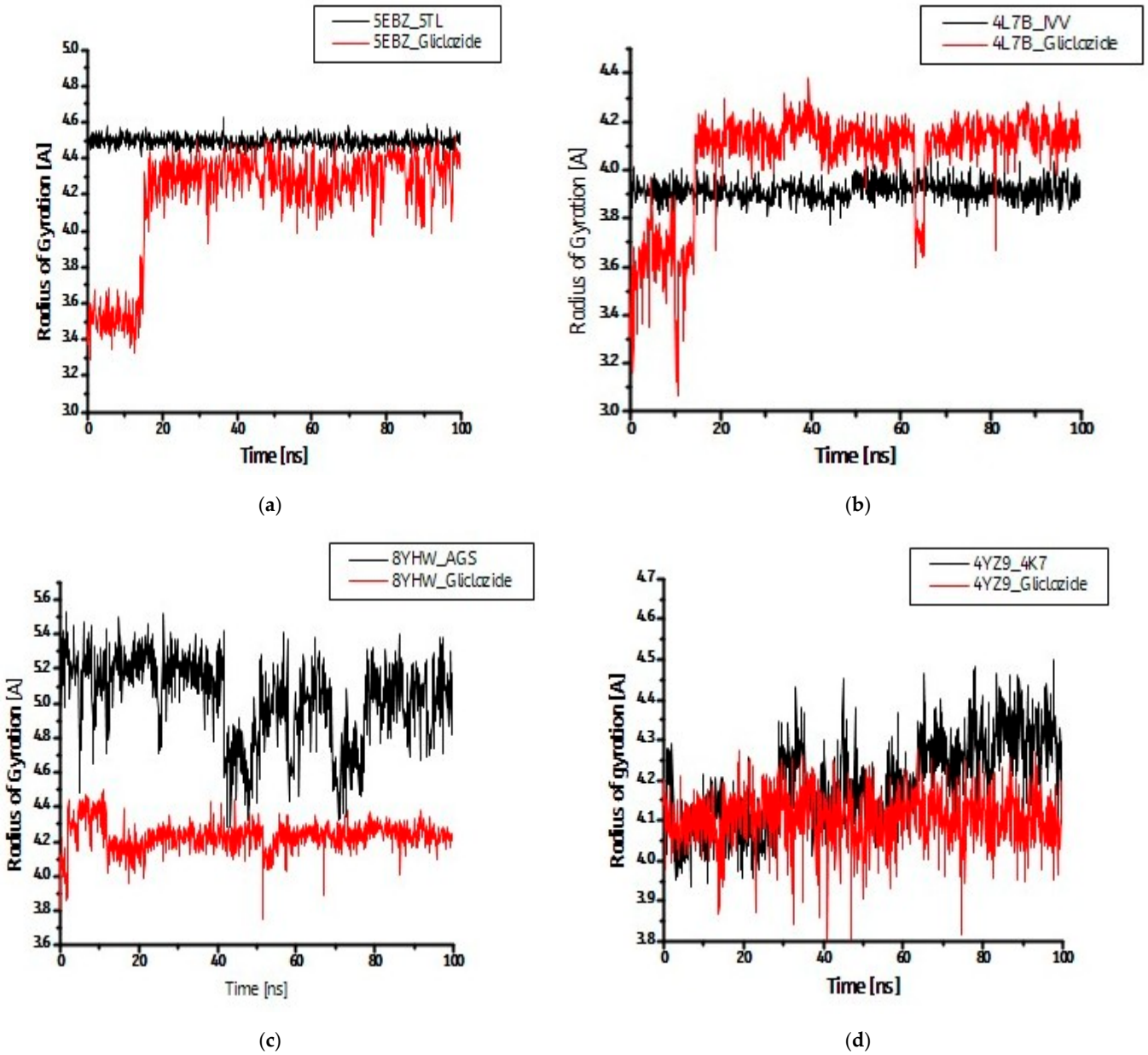


Figure 4. Radius of gyration plot as a function of simulation time-dependent analysis of the molecular dynamics trajectory of IKK-α (**a**), KKeap1 (**b**), NIK (**c**) and IRE1α (**d**). 5EBZ = IKKα, 4L7B = KKeap1, 8YHW = NIK, 4YZ9—IRE1α, 5TL = co-crystalized ligand of IKKα, IVV = co-crystalized ligand of KKeap1, AGS = co-crystalized ligand of NIK, 4K7 = co-crystalized ligand of IRE1α.

3.3. Pharmacokinetics Parameters

ADMET studies were conducted on gliclazide to obtain predicted values for parameters associated with absorption, metabolism and distribution. Results presented in Table 2 show that gliclazide had weak interactions with P-glycoprotein. Our results showed that gliclazide has a predicted logS value of 3.522 log mol/L, an indication of low solubility in water. MDCK permeability and logBBB values of value and of 2.23×10^{-6} cm/s and 0.019, respectively, were predicted for gliclazide in this study. Results from this study also showed

that in addition to CYP2C9 and CYP2C19, which are well-documented major metabolizers of gliclazide, CYP3A4 also significantly metabolizes gliclazide.

Table 2. Pharmacokinetic properties of gliclazide.

Pharmakokinetic Parameter	Value
LogS	−3.522 log mol/L
LogD7.4	1.152 log mol/L
LogP	2.114 log mol/L
Pgp-inh	0.01
Pgp-sub	0.001
Caco-2	−5.39
MDCK permeability	2.23×10^{-6} cm/s
LogBBB	0.019
PPB	95.23%
Volume of distribution	0.359 L/kg
CYP1A2-inh	0.019
CYP1A2-sub	0.24
CYP2C19-inh	0.057
CYP2C19-sub	0.942
CYP2C9-inh	0.199
CYP2C9-sub	0.895
CYP2D6-inh	0.031
CYP2D6-sub	0.256
CYP3A4-inh	0.063
CYP3A4-sub	0.916
CYP3A4-sub	0.916

BBB—blood–brain barrier; Caco-2—colon adenocarcinoma cell line; CYP—cytochromeP450 enzymes; LogD7.4—logarithm of the n-octanol/water distribution coefficients at pH 7.4; Logp—logarithm of the n-octanol/water distribution coefficient; LogS—logarithm of aqueous solubility value; MDCK—Madin−Darby Canine Kidney cells; Pgp-inh—inhibitor of P-glycoprotein; Pgp-sub—substrate of P-glycoprotein; PPB—plasma protein binding.

4. Discussion

Molecular docking is used to position the computer-generated 3-dimensional structure of small ligands into a receptor structure in a variety of orientations, conformations and positions. Searching algorithms generate possible poses, which are ranked by scoring functions [50]. This method is useful in drug discovery and medicinal chemistry by providing insights into molecular recognition. Docking has become an integral part of Computer-Aided Drug Design and Discovery (CADDD) [51]. In spite of its increasing relevance to the process of drug discovery, results from molecular docking should be taken cautiously because they do not always correlate with findings from in vivo studies. This is due to the fact that molecular docking does not completely simulate conditions in the cellular environment [52]. In this study, gliclazide was examined against four target receptors, namely, IKKα, KKeap1, NIK and IRE1α. These proteins were selected because they are mostly regulatory proteins in their respective pathways: IKKα and NIK (inflammation), KKeap1 (antioxidant) and IRE1α (endoplasmic reticulum stress), thereby making them relevant as effectors of drug action [53]. Moreover, as previously stated, these pathways are critical contributors to the pathophysiology of diabetes mellitus [25–27,34,37,38]. In addition, re-docked co-crystalized ligands of each of the proteins were used as basis of validation and comparison for binding of gliclazide to the proteins [54,55].

Noncovalent interactions between ligands and proteins are at times considered as additive and often mutually reinforcing (positively cooperative) when a ligand reduces motion within a protein [56]. There are several kinds of noncovalent interactions that contribute to the formation of a stable complex between ligand and protein. These include hydrophilic, hydrophobic, van der Waals, electrostatic, hydrogen-bonding desolvation,

etc. [57]. Results presented in Figure 1 show that the binding pockets of the proteins for gliclazide contain several polar, hydrophobic and charged amino acids, which are important for binding of ligands to proteins, and these amino acids may have contributed to the affinity and conformational stability of the binding observed in this study [58].

Various methods have been adopted to validate docking programmes and scoring functions. One of such methods is to re-dock a compound with known conformation and orientation into the active site of the target, usually a co-crystalized structure [59]. Information from the binding pocket of a co-crystalized ligand can be used to identify probable binding sites, while information on binding sites and poses is important to determine binding affinities [60,61]. A docking score is considered to be an estimate of the relative binding affinity of a ligand to a protein. More negative scores indicate stable and favourable interactions between ligands and proteins [62,63]. In this study, the resulting interactions between proteins and ligand were evaluated using XP GScore. As shown in Table 1, the predicted binding scores of gliclazide with each of the target proteins indicated appreciable binding affinities which compared favourably with those of the co-crystalized ligands. This suggests that the proteins might be relevant in contributing to the ameliorative effects of gliclazide on the pathways in which the proteins are involved.

The RMSD evaluates the structural stability of protein–ligand complexes. It also describes the measure of the changes in the conformation of a given structure over time. Low RSMD values, especially below 2 Å, are considered acceptable [64]. In the present study, the RMSD values obtained for the four protein–ligand complexes were in the range of 0.261–0.571 Å, with the lowest value observed for IRE1α and the highest values observed for IKKα. The RMSD values for the backbone atoms of the protein–ligand complexes were within reasonable ranges, indicating that the complexes were stable over the simulation time. Comparing the RMSD values of the protein–gliclazide complex for all the proteins with the proteins alone suggested that binding of gliclazide stabilized the proteins and that the ligands were stable in their binding pockets. Moreover, the observed stability is an indication of reliable docking predictions [65]. The higher RMSD values observed for the proteins (2.266–4.010 Å) are not unexpected as the proteins adopted more flexible conformations and more structural fluctuations, all of which were reduced upon ligand (gliclazide) binding [66]. Across IKKα, NIK, Keap1, and IRE1α, molecular dynamics trajectories converge on a clear conclusion: gliclazide stabilizes the protein architecture. Apo proteins sampled a broader conformational space (RMSD 2.265–4.010 Å), whereas ligand-bound complexes remained tightly constrained (0.261–0.571 Å), indicating reduced flexibility and enhanced structural integrity.

The RMSF analysis, which analyses the flexibility and local dynamics of the complexes, is a standard procedure for analyzing molecular dynamics simulations. RMSF provides important information about the behaviour of the complexes over time and can help in understanding the stability, dynamics, and binding interactions of the complexes [67]. In most cases, lower RMSF scores are indicative of protein stability, increased stability and efficient binding interactions [68]. In the present study, the RMSF values obtained for the four protein–ligand complexes were between 0.116 and 0.369 Å, with the highest value observed for KKeap1 and the lowest value observed for IRE1α. The observed lower RMSF values of ligand–protein complexes when compared with protein RMSF values (0.409–1.095 Å), analogous to the RMSD values, suggest that binding of gliclazide to the proteins might have reduced binding site flexibility and lowered fluctuations across the protein structure. Moreover, the amino acids present at the protein binding sites might have formed interactions that limit localized fluctuations in the side chains and backbones of proteins, thereby leading to more stable structures [69]. For optimum binding, an RMSF of 1–3 Å has been recommended. This implies that the binding of gliclazide to the proteins

utilized in this study can be considered optimum. It also suggests that the proteins were not unstable per se prior to ligand binding [57].

The radius of gyration gives an indication of the distribution of atoms of a molecule around its centre of mass. It gives a clue as to how compact a molecule is as well as the conformational changes that take place in the course of simulation. A lower radius of gyration value suggests that a ligand fits comfortably in the binding pocket and adopts a compact and stable conformation. Conversely, variations in the radius of gyration over the course of simulation indicate flexibility [70]. In this study, the radius of gyration of IKKα, KKeap1, NIK and IRE1α, without a bound ligand, were higher than when gliclazide was bound to them. This suggests that gliclazide was snugly bound in the binding pockets of the proteins and generated a stable protein–ligand complex. These results align with the RMSD data, both of which demonstrated that gliclazide was stably bound to the proteins targeted in this study.

In the present study, pharmacokinetic parameters of gliclazide bordering on absorption and distribution (solubility), transport (plasma protein binding) and metabolism (CYPs) were evaluated and their results are presented in Table 2. Knowledge of the pharmacokinetic properties of drugs, encompassing absorption, distribution, metabolism, excretion and toxicity, has become very important as it helps to facilitate drug discovery while also optimizing and preserving currently available drugs [71,72]. The absorption, bioavailability and efficacy of drugs are affected by their aqueous solubility, and most drugs strike a balance between reasonable aqueous solubility and required hydrophobicity for reasonable passage across the membrane. The solubility of compounds is usually denoted by logS, with about 85% of drugs having logS values in the range of −1 to −5 log mol/L. The hydrophilicity of drugs increases with increasing logS values [73]. The predicted logS value for gliclazide in this study was 3.522 log mol/L, suggesting that it has a low aqueous solubility. The expected limitation to gliclazide's effectiveness due to its logS value is, however, countered via methods which include reduction in the particle size of the drug and the inclusion of a hydrophilic matrix, which forms a gel that gradually releases the drug over a 24 h period [74].

Lipophilicity is usually quantitatively expressed as either partition coefficient (logP) or distribution coefficient (logD). However, logD at physiological pH (logD7.4), which factors in the pH and ionization forms of drugs, is considered a more relevant assessment of drugs' lipophilicity than logP [75]. Drugs enter cells more efficiently if logD7.4 is greater than 1 but less than 3–5 [76]. Moreover, a logP value between 0 and 5 has been reported to be optimal for orally administered drugs, with lipophilicity increasing as the logP value increases. In this study, the predicted LogD7.4 and LogP values for gliclazide are, respectively, 1.152 and 2.114 log mol/L, which supports the hydrophobic characteristic of gliclazide, its designation as a class II drug by Biopharmaceutical Classification System (due to low solubility and high permeability across membranes) and its extensive binding to plasma proteins [54,77]. Our results contrast with earlier studies which reported an experimental logP value of 2.6 log mol/L and predicted logP values of 1.7 and 1.52 for gliclazide [78,79].

The prediction that gliclazide interacts weakly with P-glycoprotein (Pgp), either as inhibitor or substrate, is noteworthy. This is because Pgp is a membrane transporter that plays a crucial role in drug efflux from cells, thereby reducing their bioavailability [80,81]. This finding suggests that gliclazide may not be subject to efflux, potentially leading to improved bioavailability. Caco-2 cells are often used as a model to predict in vivo drug permeability across membranes [82]. In this study, the predicted Caco-2 permeability for gliclazide was −5.386 log cm/s, suggesting that gliclazide may have efficient passive diffusion across intestinal cell membranes. The predicted Caco-2 permeability in this study is closer to the reference value of −6.0 [78], but is far removed from the values reported in earlier

studies, which ranged from 0.32 log cm/s (low permeability) [83] to −4.602 log cm/s [78]. On the other hand, the MDCK permeability value of 2.23×10^{-6} cm/s indicates moderate uptake efficiency, implying that gliclazide may not be efficiently transported across certain biological barriers, such as the blood–brain barrier (BBB). This observation correlates with a logBBB value of 0.019 observed for gliclazide in this study and is supported by earlier studies which reported that gliclazide does not freely cross the BBB, a situation that may be advantageous in avoiding potential central nervous system (CNS) side effects if the drug's target is peripheral [77,84]. The inability of gliclazide to cross the BBB aligns with its characteristics, relating to its low solubility and extensive binding to plasma proteins.

The high plasma protein binding (PPB) of 95.23% suggests that a significant portion of gliclazide is bound to plasma proteins. This value corresponds to an earlier reported value of 94% [77]. While this binding can enhance drug stability and prolong the drug's action, it may also limit the fraction of free drug available to interact with its target and affect pharmacokinetics. The volume of distribution (VD) value of 0.359 L/kg indicates a relatively small distribution volume, which may impact the drug's distribution in the body and its tissue penetration. This observation is in tandem with an earlier study which reported high protein binding and a small volume of distribution for gliclazide in both diabetic patients and healthy individuals [77,85,86]. The possible effect of gliclazide's low VD and extensive binding to plasma proteins is circumvented, especially in the modified release form, by a steady release of unbound drug from the plasma proteins to replace the metabolized ones [87]. Results from this study suggest that CYP2C9 (CYP2C9-sub of 0.895) and CYP2C19 (CYP2C19-sub of 0.942) are major metabolizers of gliclazide, findings corroborated by earlier studies [88]. However, in this study, CYP3A4, which was earlier reported to be a minor metabolizer of gliclazide, appeared to contribute significantly to gliclazide metabolism (CYP3A4-sub-0.916) [89–91]. This information is crucial for understanding potential drug–drug interactions and the involvement of these enzymes in the drug's clearance and metabolism. An elaborate comparison of the values obtained for pharmacokinetics evaluation in this study was not performed based on the inherent variations in such values among individuals [92].

Findings from this study predict that gliclazide interacted reasonably with IKKα, KKeap1, NIK and IRE1α, thereby underscoring the reported antioxidant, anti-inflammatory and anti-ER stress properties [93–95]. The biological activities of gliclazide on these pathways might be via its interaction with the proteins evaluated in this study. The extrapancreatic effects of gliclazide and its predicted pharmacokinetic properties in this study, especially its lipophilicity, have been attributed to its unique aminoazabicyclo-octane ring, which possesses direct radical scavenging and antioxidant activities [96].

5. Conclusions

This study predicted that gliclazide showed appreciable binding affinity and stable interactions with IKKα, NIK, KKeap1 and IRE1α. The interaction of gliclazide with these proteins, which have been implicated in the pathophysiology of diabetes and are critical regulators of their respective pathways, might be the mechanism through which it exerts its amelioration of oxidative stress and by extension, its amelioration of inflammation and ER stress in the diabetes state. This is important because of the cause-and-effect relationships that exist among the three biochemical phenomena. The pharmacokinetic properties of gliclazide as observed in this study also highlight its pharmacological effects. Parameters pertaining to absorption, distribution, metabolism and bioavailability, which were evaluated, aligns with the established characteristics of gliclazide. However, findings from this study suggested that CYP3A4 might contribute to the metabolism of gliclazide, an observation that does not conform to the literature. Further (in vivo) studies, particularly

on its aminoazabicyclo-octane ring and its contribution to the antioxidant properties of gliclazide, are required to validate the outcomes of this study. In spite of the substance of this study, it is limited by the lack of either in vitro or in vivo studies.

Author Contributions: Conceptualization, O.T.O., A.O.A. and M.N.; methodology, O.T.O., A.O.A. and A.O.O.; investigation, O.T.O., B.A.O. and J.O.U.; supervision, S.L.L. and M.N.; writing—original draft, B.A.O. and J.O.U.; writing—review and editing, A.O.O. and S.L.L. All authors have read and agreed to the published version of the manuscript.

Funding: This research received no external funding.

Institutional Review Board Statement: Not applicable.

Informed Consent Statement: Not applicable.

Data Availability Statement: The original contributions presented in this study are included in the article. Further inquiries can be directed to the corresponding author.

Conflicts of Interest: The authors declare no conflicts of interest.

Abbreviations

The following abbreviations are used in this manuscript:

AMBER	Assisted model building with energy refinement
BBB	Blood–brain barrier
ATF6	Activating transcription factor-6
Caco-2	Colon adenocarcinoma cell line
CNS	Central nervous system
CYP	Cytochrome P_{450}
ER	Endoplasmic reticulum
GDM	Gestational diabetes
GRP78	Glucose-regulated protein-78
IKK	Inhibitor of nuclear factor kappa-B kinase
IRE1α	Inositol-requiring enzyme-1alpha
Keap1	Kelch-like ECH-associated protein 1
LogD7.4	Logarithm of the n-octanol/water distribution coefficients at pH 7.4
Logp	Logarithm of the n-octanol/water distribution coefficient
LogS	Logarithm of aqueous solubility value
MDCK	Madin−Darby Canine Kidney cells
MM-GBSA	Molecular Mechanics/generalized-born/surface area
NF-κB	Nuclear factor kappa-light-chain-enhancer of activated B cells
NIK	NF-kappa-B-inducing kinase
Nrf2	Nuclear factor erythroid 2-related factor2
PDB	Protein databank
Pgp-inh	Inhibitor of P-glycoprotein
Pgp-sub	Substrate of P-glycoprotein
PPB	Plasma protein binding
PERK	Protein Kinase-R-like ER kinase
RMSD	Root mean-square deviation
RMSF	Root mean-square fluctuation
TRAF2/3	Tumour necrosis factor receptor-associated factor 2 and 3
T1DM	Type 1 diabetes
T2DM	Type 2 diabetes
UPR	Unfolded protein response
VD	Volume of distribution
WHO	World Health Organization
XP	Extra precision

References

1. World Health Organization. *Global Report on Diabetes 2016*; WHO: Geneva, Switzerland, 2016.
2. World Health Organization. *Noncommunicable Diseases Country Profile 2018*; WHO: Geneva, Switzerland, 2018.
3. International Diabetes Federation. *IDF Diabetes Atlas*, 8th ed.; International Diabetes Federation: Brussels, Belgium, 2017.
4. Saeedi, P.; Petersohn, I.; Salpea, P.; Malanda, B.; Karuranga, S.; Unwin, N.; Colagiuri, S.; Guariguata, L.; Motala, A.A.; Ogurtsova, K.; et al. Global and regional diabetes prevalence estimates for 2019 and projections for 2030 and 2045: Results from the International Diabetes Federation Diabetes Atlas, 9th edition. *Diabetes Res. Clin. Pract.* **2019**, *157*, 107843. [CrossRef]
5. Tsalamandris, S.; Antonopoulos, A.S.; Oikonomou, E.; Papamikroulis, G.A.; Vogiatzi, G.; Papaioannou, S.; Deftereos, S.; Tousoulis, D. The Role of Inflammation in Diabetes: Current Concepts and Future Perspectives. *Eur. Cardiol. Rev.* **2019**, *14*, 50–59. [CrossRef]
6. Obafemi, T.O.; Alfa, J.A.; Obafemi, B.A.; Jaiyesimi, K.F.; Olasehinde, O.R.; Adewale, O.B.; Akintayo, C.O.; Adu, I.A. Comparative effect of metformin and gliclazide on expression of some genes implicated in oxidative stress, endoplasmic reticulum stress, and inflammation in liver and pancreas of type 2 diabetic rats. *Comp. Clin. Pathology* **2024**, *33*, 115–125. [CrossRef]
7. Christensen, A.A.; Gannon, M. The Beta Cell in Type 2 Diabetes. *Curr. Diabetes Rep.* **2019**, *19*, 81. [CrossRef] [PubMed]
8. Galicia-Garcia, U.; Benito-Vicente, A.; Jebari, S.; Larrea-Sebal, A.; Siddiqi, H.; Uribe, K.B.; Ostolaza, H.; Martín, C. Pathophysiology of Type 2 Diabetes Mellitus. *Int. J. Mol. Sci.* **2020**, *21*, 6275. [CrossRef] [PubMed]
9. Reuter, S.; Gupta, S.C.; Chaturvedi, M.M.; Aggarwal, B.B. Oxidative stress, inflammation, and cancer: How are they linked? *Free Radic. Biol. Med.* **2010**, *49*, 1603–1616. [CrossRef]
10. Chong, W.C.; Shastri, M.D.; Eri, R. Endoplasmic Reticulum Stress and Oxidative Stress: A Vicious Nexus Implicated in Bowel Disease Pathophysiology. *Int. J. Mol. Sci.* **2017**, *18*, 771. [CrossRef] [PubMed]
11. Oguntibeju, O.O. Type 2 diabetes mellitus, oxidative stress and inflammation: Examining the links. *Int. J. Physiol. Pathophysiol. Pharmacol.* **2019**, *11*, 45–63.
12. Polavarapu, N.K.; Kale, R.; Sethi, B.; Sahay, R.K.; Phadke, U.; Ramakrishnan, S.; Mane, A.; Mehta, S.; Shah, S. Effect of Gliclazide or Gliclazide plus Metformin Combination on Glycemic Control in Patients with T2DM in India: A Real-World, Retrospective, Longitudinal, Observational Study from Electronic Medical Records. *Drugs Real World Outcomes* **2020**, *7*, 271–279. [CrossRef]
13. World Health Organization. *Model List of Essential Medicines*, 21st ed.; World Health Organization: Geneva, Switzerland, 2019.
14. Signorini, A.M.; Fondelli, C.; Renzoni, E.A.; Puccetti, C.; Gragnoli, G.; Giorgi, G. Antioxidant effects of gliclazide, glibenclamide, and metformin in patients with type 2 diabetes mellitus. *Curr. Ther. Res.* **2002**, *63*, 411–420. [CrossRef]
15. Bishnoi, A.; Sur, A.; Gonsalves, B.; Atri, B.; Goswami, S.; Ravindranath, V.; Patel, V.; Prajapati, H.; Shah, D. Taking a Closer Look at Gliclazide—Benefits Beyond Glycemic Control. *Int. J. Diabetes Technol.* **2025**, *4*, 49–54. [CrossRef]
16. Zhang, Q.; Lenardo, M.J.; Baltimore, D. 30 years of NF-kappaB: A blossoming of relevance to human pathobiology. *Cell* **2017**, *168*, 37–57. [CrossRef]
17. Wang, Y.; Rui, L. The Druggable Target Potential of NF-κB-Inducing Kinase (NIK) in Cancer. *Int. J. Transl. Med.* **2025**, *5*, 1. [CrossRef]
18. Qing, G.; Qu, Z.; Xiao, G. Stabilization of basally translated NF-kappaB-inducing kinase (NIK) protein functions as a molecular switch of processing of NF-kappaB2 p100. *J. Biol. Chem.* **2005**, *280*, 40578–40582. [CrossRef] [PubMed]
19. Meyerovich, K.; Ortis, F.; Cardozo, A.K. The non-canonical NF-κB pathway and its contribution to β-cell failure in diabetes. *J. Mol. Endocrinol.* **2018**, *61*, F1–F6. [CrossRef]
20. Ghosh, G.; Wang, V.Y. Origin of the Functional Distinctiveness of NFκB/p52. *Front. Cell Dev. Biol.* **2021**, *9*, 764164. [CrossRef]
21. Fusco, A.J.; Huang, D.B.; Miller, D.; Wang, V.Y.; Vu, D.; Ghosh, G. NF-kappaB p52:RelB heterodimer recognizes two classes of kappaB sites with two distinct modes. *EMBO Rep.* **2009**, *10*, 152–159. [CrossRef] [PubMed]
22. Prescott, J.A.; Balmanno, K.; Mitchell, J.P.; Okkenhaug, H.; Cook, S.J. IKKα plays a major role in canonical NF-κB signalling in colorectal cells. *Biochem. J.* **2022**, *479*, 305–325. [CrossRef] [PubMed]
23. Haselager, M.V.; Eldering, E. The therapeutic potential of targeting NIK in B cell. malignancies. *Front. Immunol.* **2022**, *13*, 930986. [CrossRef]
24. Yamamoto, Y.; Yin, M.J.; Gaynor, R.B. IkappaB kinase alpha (IKKalpha) regulation of IKKbeta kinase activity. *Mol. Cell Biol.* **2000**, *20*, 3655–3666. [CrossRef]
25. Cai, D.; Yuan, M.; Frantz, D.F.; Melendez, P.A.; Hansen, L.; Lee, J.; Shoelson, S.E. Local and systemic insulin resistance resulting from hepatic activation of IKK-β and NF-kB. *Nat. Med.* **2005**, *11*, 183–190. [CrossRef]
26. Ke, B.; Zhao, Z.; Ye, X.; Gao, Z.; Manganiello, V.; Wu, B.; Ye, J. Inactivation of NF-kB p65 (RelA) in liver improves insulin sensitivity and inhibits cAMP/PKA pathway. *Diabetes* **2015**, *64*, 3355–3362. [CrossRef]
27. Hernandez, R.; Zhou, C. Recent Advances in Understanding the Role of IKKb in Cardiometabolic Diseases. *Front. Cardiovasc. Med.* **2021**, *8*, 752337. [CrossRef]
28. Gardner, B.M.; Walter, P. Unfolded proteins are Ire1-activating ligands that directly induce the unfolded protein response. *Science* **2011**, *333*, 1891–1894. [CrossRef]

29. Carrara, M.; Prischi, F.; Nowak, P.R.; Kopp, M.C.; Ali, M.M. Non-canonical binding of BiP ATPase domain to Ire1 and Perk is dissociated by unfolded protein CH1 to initiate ER stress signaling. *eLife* **2015**, *4*, e03522. [CrossRef]
30. Ghosh, R.; Colon-Nrgron, K.; Papa, F.R. Endoplasmic reticulum stress, degeneration of pancreatic islet β-cells, and therapeutic modulation of the unfolded protein response in diabetes. *Mol. Metab.* **2019**, *27*, S60–S68. [CrossRef]
31. Herlea-Pana, O.; Eeda, V.; Undi, R.B.; Lim, H.Y.; Wang, W. Pharmacological Inhibition of Inositol Requiring Enzyme 1a RNase Activity Protects Pancreatic Beta Cell and Improves Diabetic Condition in Insulin Mutation-Induced Diabetes. *Front. Endocrinol.* **2021**, *12*, 749879. [CrossRef] [PubMed]
32. Cai, J.; Zhang, X.; Chen, P.; Li, Y.; Liu, S.; Liu, Q.; Zhang, H.; Wu, Z.; Song, K.; Liu, J.; et al. The ER stress sensor inositol-requiring enzyme 1α in Kupffer cells promotes hepatic ischemia-reperfusion injury. *J. Biol. Chem.* **2022**, *298*, 101532. [CrossRef] [PubMed]
33. Lee, J.-H.; Lee, J. Endoplasmic Reticulum (ER) Stress and Its Role in Pancreatic β-Cell Dysfunction and Senescence in Type 2 Diabetes. *Int. J. Mol. Sci.* **2022**, *23*, 4843. [CrossRef]
34. He, Z.; Liu, Q.; Wang, Y.; Zhao, B.; Zhang, L.; Yang, X.; Wang, Z. The role of endoplasmic reticulum stress in type 2 diabetes mellitus mechanisms and impact on islet function. *PeerJ* **2025**, *13*, e19192. [CrossRef] [PubMed]
35. Uruno, A.; Yagishita, Y.; Yamamoto, M. The Keap1-Nrf2 system and diabetes mellitus. *Arch. Biochem. Biophys.* **2015**, *566*, 76–84. [CrossRef]
36. Long, M.; de la Vega, M.R.; Wen, Q.; Bharara, M.; Jiang, T.; Zhang, R.; Zhou, S.; Wong, P.K.; Wondrak, G.T.; Zheng, H.; et al. An essential role of NRF2 in diabetic wound healing. *Diabetes* **2016**, *65*, 780–793. [CrossRef]
37. Lu, M.C.; Ji, J.A.; Jiang, Z.Y.; You, Q.D. The Keap1-Nrf2-ARE Pathway as a Potential Preventive and Therapeutic Target: An Update. *Med. Res. Rev.* **2016**, *36*, 924–963. [CrossRef]
38. Li, W.; Kong, A.N. Molecular mechanisms of Nrf2-mediated antioxidant response. *Mol. Carcinog.* **2009**, *48*, 91–104. [CrossRef] [PubMed]
39. Ibrahim, M.; Munir, S.; Ahmed, S.; Chughtai, A.H.; Ahmad, W.; Khan, J.; Murtey, M.D. Gliclazide in Binary and Ternary Systems Improves Physicochemical Properties, Bioactivity, and Antioxidant Activity. *Oxidative Med. Cell. Longev.* **2022**, *25*, 2100092. [CrossRef]
40. ADVANCE Collaborative Group. Intensive blood glucose control and vascular outcomes in patients with type 2 diabetes. *N. Engl. J. Med.* **2008**, *358*, 2560–2572. [CrossRef]
41. Polley, S.; Passos, D.O.; Huang, D.; Mulero, M.C.; Mazumder, A.; Biswas, T.; Verma, I.M.; Lyumkis, D.; Ghosh, G. Structural Basis for the Activation of IKK1/α. *Cell Rep.* **2016**, *17*, 1907–1914. [CrossRef]
42. Jnoff, E.; Albrecht, C.; Barker, J.J.; Barker, O.; Beaumont, E.; Bromidge, S.; Brookfield, F.; Brooks, M.; Bubert, C.; Ceska, T.; et al. Binding mode and structure-activity relationships around direct inhibitors of the Nrf2-Keap1 complex. *ChemMedChem* **2014**, *9*, 699–705. [CrossRef] [PubMed]
43. Wang, F.; Cheng, W.; Lv, Z.; Meng, Q.; Xu, Y. The crystal structure of NF-κB-inducing kinase (NIK) from Biortus. In *Full wwPDB X-ray Structure Validation Report*; Worldwide Protein Data Bank: New Brunswick, NJ, USA, 2024.
44. Concha, N.O.; Smallwood, A.; Bonnette, W.; Totoritis, R.; Zhang, G.; Federowicz, K.; Yang, J.; Qi, H.; Chen, S.; Campobasso, N.; et al. Long-Range Inhibitor-Induced Conformational Regulation of Human IRE1α Endoribonuclease Activity. *Mol. Pharmacol.* **2015**, *88*, 1011–1023. [CrossRef] [PubMed]
45. Berman, H.M.; Battistuz, T.; Bhat, T.N.; Bluhm, W.F.; Bourne, P.E.; Burkhardt, K.; Feng, Z.; Gilliland, G.L.; Iype, L.; Jain, S.; et al. The Protein Data Bank. *Acta Crystallogr. Sect. D Biol. Crystallogr.* **2002**, *58*, 899–907. [CrossRef]
46. Available online: https://www.rcsb.org/structure/5EBZ (accessed on 19 August 2025).
47. Available online: https://www.rcsb.org/structure/4L7B (accessed on 19 August 2025).
48. Available online: https://www.rcsb.org/structure/8YHW (accessed on 19 August 2025).
49. Available online: https://www.rcsb.org/structure/4YZ9 (accessed on 19 August 2025).
50. Liu, Z.; Liu, Y.; Zeng, G.; Shao, B.; Chen, M.; Li, Z. Application of molecular docking for the degradation of organic pollutants in the environmental remediation: A review. *Chemosphere* **2018**, *203*, 139–150. [CrossRef] [PubMed]
51. Jakhar, R.; Dangi, M.; Khichi, A.; Chhillar, A.K. Relevance of molecular docking studies in drug designing. *Curr. Bioinform.* **2020**, *15*, 270–278. [CrossRef]
52. Cava, C.; Castiglioni, I. Integration of Molecular Docking and In Vitro Studies: A Powerful Approach for Drug Discovery in Breast Cancer. *Appl. Sci.* **2020**, *10*, 6981. [CrossRef]
53. Li, Y.; Li, W.; Chen, X.; Jiang, H.; Sun, J.; Chen, H.; Lv, S. Integrated analysis identifies interaction patterns between small molecules and pathways. *Biomed Res. Int.* **2014**, *2014*, 931825. [CrossRef]
54. Patel, C.N.; Georrge, J.J.; Modi, K.M.; Narechania, M.B.; Patel, D.P.; Gonzalez, F.J.; Pandya, H.A. Pharmacophore-based virtual screening of catechol-o-methyltransferase (COMT) inhibitors to combat Alzheimer's disease. *J. Biomol. Struct. Dyn.* **2018**, *36*, 3938–3957. [CrossRef]

55. Ogbodo, U.C.; Enejoh, O.A.; Okonkwo, C.H.; Gnanasekar, P.; Gachanja, P.W.; Osata, S.; Atanda, H.C.; Iwuchukwu, E.A.; Achilonu, I.; Awe, O.I. Computational identification of potential inhibitors targeting cdk1 in colorectal cancer. *Front. Chem.* **2023**, *11*, 1264808. [CrossRef]
56. Williams, D.H.; Stephens, E.; O'Brien, D.P.; Zhou, M. Understanding noncovalent interactions: Ligand binding energy and catalytic efficiency from ligand-induced reductions in motion within receptors and enzymes. *Angew. Chem. Int. Ed.* **2004**, *43*, 6596–6616. [CrossRef]
57. Mohanty, M.; Mohanty, P.S. Molecular docking in organic, inorganic, and hybrid systems: A tutorial review. *Monatshefte Für Chem.* **2023**, *154*, 683–707. [CrossRef]
58. Desantis, F.; Miotto, M.; Di Rienzo, L.; Milanetti, E.; Ruocco, G. Spatial organization of hydrophobic and charged residues affects protein thermal stability and binding affinity. *Sci. Rep.* **2022**, *12*, 12087. [CrossRef]
59. Hevener, K.E.; Zhao, W.; Ball, D.M.; Babaoglu, K.; Qi, J.; White, S.W.; Lee, R.E. Validation of molecular docking programs for virtual screening against dihydropteroate synthase. *J. Chem. Inf. Model.* **2009**, *49*, 444–460. [CrossRef]
60. Oshima, H.; Re, S.; Sugita, Y. Prediction of Protein-Ligand Binding Pose and Affinity Using the gREST+FEP Method. *J. Chem. Inf. Model.* **2020**, *60*, 5382–5394. [CrossRef]
61. Tran-Nguyen, V.K.; Camproux, A.C. Computational modeling of protein-ligand interactions: From binding site identification to pose prediction and beyond. *Curr. Opin. Struct. Biol.* **2025**, *95*, 103152. [CrossRef] [PubMed]
62. Alsedfy, M.Y.; Ebnalwaled, A.A.; Moustafa, M.; Said, A.H. Investigating the binding affinity, molecular dynamics, and ADMET properties of curcumin-IONPs as a mucoadhesive bioavailable oral treatment for iron deficiency anemia. *Sci. Rep.* **2024**, *14*, 22027. [CrossRef]
63. Issa, N.T.; Badiavas, E.V.; Schürer, S. Research Techniques Made Simple: Molecular Docking in Dermatology—A Foray into In Silico Drug Discovery. *J. Investig. Dermatol.* **2019**, *139*, 2400–2408.e1. [CrossRef]
64. Aziz, M.; Ejaz, S.A.; Zargar, S.; Akhtar, N.; Aborode, A.T.; Wani, T.A.; Batiha, G.E.; Siddique, F.; Alqarni, M.; Akintola, A.A. Deep Learning and Structure-Based Virtual Screening for Drug Discovery against NEK7: A Novel Target for the Treatment of Cancer. *Molecules* **2022**, *27*, 4098. [CrossRef]
65. Trezza, A.; Visibelli, A.; Roncaglia, B.; Barletta, R.; Iannielli, S.; Mahboob, L.; Spiga, O.; Santucci, A. Unveiling Dynamic Hotspots in Protein–Ligand Binding: Accelerating Target and Drug Discovery Approaches. *Int. J. Mol. Sci.* **2025**, *26*, 3971. [CrossRef]
66. Amini, F.; Abbas, K.I.; Ghasemi, J.B. Molecular modeling approach in design of new scaffold of α-glucosidase inhibitor as antidiabetic drug. *Biochem. Biophys. Rep.* **2025**, *42*, 101995. [CrossRef] [PubMed]
67. Mangat, H.K.; Rani, M.; Pathak, R.K.; Yadav, I.S.; Utreja, D.; Chhuneja, P.K.; Chhuneja, P. Virtual screening, molecular dynamics and binding energy-MM-PBSA studies of natural compounds to identify potential EcR inhibitors against *Bemisia tabaci* Gennadius. *PLoS ONE* **2022**, *17*, e0261545. [CrossRef]
68. Hassan, A.M.; Gattan, H.S.; Faizo, A.A.; Alruhaili, M.H.; Alharbi, A.S.; Bajrai, L.H.; AL-Zahrani, I.A.; Dwivedi, V.D.; Azhar, E.I. Evaluating the Binding Potential and Stability of Drug-like Compounds with the Monkeypox Virus VP39 Protein Using Molecular Dynamics Simulations and Free Energy Analysis. *Pharmaceuticals* **2024**, *17*, 1617. [CrossRef] [PubMed]
69. Fatriansyah, J.F.; Rizqillah, R.K.; Yandi, M.Y.; Fadilah, S.M. Molecular docking and dynamics studies on propolis sulabiroin-A as a potential inhibitor of SARS-CoV-2. *J. King Saud. Univ. Sci.* **2022**, *34*, 101707. [CrossRef]
70. Bouone, Y.O.; Bouzina, A.; Djemel, A.; Bardaweel, S.K.; Ibrahim-Ouali, M.; Bakchiche, B.; Benaceur, F.; Aouf, N.E. Investigation of the anticancer activity of modified 4-hydroxyquinolone analogues: In vitro and in silico studies. *RSC Adv.* **2025**, *15*, 3704–3720. [CrossRef]
71. Vuppala, P.K.; Janagam, D.R.; Balabathula, P. Importance of ADME and Bioanalysis in the Drug Discovery. *J. Bioequivalence Bioavailab.* **2013**, *5*, e31. [CrossRef]
72. Palmer, M.E.; Andrews, L.J.; Abbey, T.C.; Dahlquist, A.E.; Wenzler, E. The importance of pharmacokinetics and pharmacodynamics in antimicrobial drug development and their influence on the success of agents developed to combat resistant gram negative pathogens: A review. *Front. Pharmacol.* **2022**, *13*, 888079. [CrossRef]
73. Jorgensen, W.L.; Duffy, E.M. Prediction of drug solubility from structure. *Adv. Drug Deliv. Rev.* **2002**, *54*, 355–366. [CrossRef] [PubMed]
74. Nasr, M.; Almawash, S.; Al Saqr, A.; Bazeed, A.Y.; Saber, S.; Elagamy, H.I. Bioavailability and Antidiabetic Activity of Gliclazide-Loaded Cubosomal Nanoparticles. *Pharmaceuticals* **2021**, *14*, 786. [CrossRef] [PubMed]
75. Wang, Y.; Xiong, J.; Xiao, F.; Zhang, W.; Gheng, K.; Rao, J.; Niu, B. LogD7.4 prediction enhanced by transferring knowledge from chromatographic retention time, microscopic pKa and logP. *J. Cheminform.* **2023**, *15*, 76. [CrossRef] [PubMed]
76. Waring, M.J. Defining optimum lipophilicity and molecular weight ranges for drug candidates—Molecular weight dependent lower logD limits based on permeability. *Bioorg Med. Chem. Lett.* **2009**, *19*, 2844–2851. [CrossRef]
77. Sarkar, A.; Tiwari, A.; Bhasin, P.S.; Mitra, M. Pharmacological and Pharmaceutical Profile of Gliclazide: A Review. *J. Appl. Pharm. Sci.* **2011**, *1*, 11–19.

78. Mapa, B.d.C.; Araújo, L.U.; Silva-Barcellos, N.M.; Caldeira, T.G.; Souza, J. Gliclazide: Biopharmaceutics Characteristics to Discuss the Biowaiver of Immediate and Extended Release Tablets. *Appl. Sci.* **2020**, *10*, 7131. [CrossRef]
79. Ramanathan, K.; Karthick, H.; Arun, N. Structure Based Drug Designing for Diabetes Mellitus. *J. Proteom. Bioinform.* **2010**, *3*, 310–313. [CrossRef]
80. Lin, J.H.; Yamazaki, M. Role of P-Glycoprotein in Pharmacokinetics. *Clin. Pharmacokinet.* **2003**, *42*, 59–98. [CrossRef]
81. Gandla, K.; Islam, F.; Zehravi, M.; Karunakaran, A.; Sharma, I.; Haque, M.A.; Kumar, S.; Pratyush, K.; Dhawale, S.A.; Nainu, F.; et al. Natural polymers as potential P-glycoprotein inhibitors: Pre-ADMET profile and computational analysis as a proof of concept to fight multidrug resistance in cancer. *Heliyon* **2023**, *24*, e19454. [CrossRef]
82. Keemink, J.; Bergström, C.A.S. Caco-2 Cell Conditions Enabling Studies of Drug Absorption from Digestible Lipid-Based Formulations. *Pharm. Res.* **2018**, *35*, 74. [CrossRef]
83. Đanić, M.; Pavlović, N.; Zaklan, D.; Stanimirov, B.; Lazarević, S.; Al-Salami, H.; Mikov, M. Computational studies for pre-evaluation of pharmacological profile of gut microbiota produced gliclazide metabolites. *Front. Pharmacol.* **2024**, *15*, 1492284. [CrossRef]
84. Lalic-Popovic, M.; Vasovic, V.; Milijasevic, B.; Golocorbin-Kon, S.; Al-Salami, H.; Mikov, M. Deoxycholic acid as a modifier of the permeation of gliclazide through the blood brain barrier of a rat. *J. Diabetes Res.* **2013**, *2013*, 598–603. [CrossRef]
85. Pop, D.I.; Oroian, M.; Bhardwaj, S.; Marcovici, A.; Khuroo, A.; Kochhar, R.; Vlase, L. Bioequivalence of two formulations of gliclazide in a randomized crossover study in healthy caucasian subjects under fasting conditions. *Clin. Pharmacol. Drug Dev.* **2019**, *8*, 16–21. [CrossRef]
86. Nazief, A.M.; Hassaan, P.S.; Khalifa, H.M.; Sokar, M.S.; El-Kamel, A.H. Lipid-Based Gliclazide Nanoparticles for Treatment of Diabetes: Formulation, Pharmacokinetics, Pharmacodynamics and Subacute Toxicity Study. *Int. J. Nanomed.* **2020**, *15*, 1129–1148. [CrossRef]
87. McGavin, J.K.; Perry, C.M.; Goa, K.L. Gliclazide modified release. *Drugs* **2002**, *62*, 1357–1364; discussion 1365–1366. [CrossRef]
88. Elliot, D.J.; Lewis, B.C.; Gillam, E.M.; Birkett, D.J.; Gross, A.S.; Miners, J.O. Identification of the human cytochromes P450 catalysing the rate-limiting pathways of gliclazide elimination. *Br. J. Clin. Pharmacol.* **2007**, *64*, 450–457. [CrossRef] [PubMed]
89. Mastan, S.K.; Chaitanya, G.; Reddy, K.R.; Kumar, K.E. An appraisal to the special sulphonylurea: Gliclazide. *Pharmacologyonline* **2009**, *1*, 254–269.
90. Mastan, S.K.; Kumar, K.E. Influence of atazanavir on the pharmacodynamics and pharmacokinetics of gliclazide in animal models. *Int. J. Diabetes Mellit.* **2010**, *2*, 56–60. [CrossRef]
91. Wang, K.; Yang, A.; Shi, M.; Tam, C.C.H.; Lau, E.S.H.; Fan, B.; Lim, C.K.P.; Lee, H.M.; Kong, A.P.S.; Luk, A.O.Y.; et al. CYP2C19 Loss-of-function Polymorphisms are Associated with Reduced Risk of Sulfonylurea Treatment Failure in Chinese Patients with Type 2 Diabetes. *Clin. Pharmacol. Ther.* **2022**, *111*, 461–469. [CrossRef] [PubMed]
92. Eusuf, D.V.; Thomas, E. Pharmacokinetic variation. *Anaesth. Intensive Care Med.* **2022**, *23*, 50–53. [CrossRef]
93. O'Brien, R.C.; Luo, M.; Balazs, N.; Mercuri, J. In vitro and in vivo antioxidant properties of gliclazide. *J. Diabetes Its Complicat.* **2000**, *14*, 201–206. [CrossRef] [PubMed]
94. Sun, W.; Bi, Y.; Liang, H.; Cai, M.; Che, X.; Zhu, Y.; Liao, L.; Weng, J. The effects of insulin and gliclazide therapy on endoplasmic reticulum stress and insulin sensitivity in liver of type 2 diabetic rats. *Chin. J. Integr. Med.* **2012**, *51*, 638–641.
95. Mafra, C.A.D.; Vasconcelos, R.C.; de Medeiros, C.A.C.; Leitão, R.F.C.; Brito, G.A.C.; Costa, D.V.D.; Guerra, G.C.B.; de Araújo, R.F.; Medeiros, A.C.; de Araújo, A.A. Gliclazide Prevents 5-FU-Induced Oral Mucositis by Reducing Oxidative Stress, Inflammation, and P-Selectin Adhesion Molecules. *Front. Physiol.* **2019**, *26*, 327. [CrossRef] [PubMed]
96. Jennings, P.E. Vascular benefits of gliclazide beyond glycemic control. *Metabolism* **2000**, *49*, 17–20. [CrossRef]

Disclaimer/Publisher's Note: The statements, opinions and data contained in all publications are solely those of the individual author(s) and contributor(s) and not of MDPI and/or the editor(s). MDPI and/or the editor(s) disclaim responsibility for any injury to people or property resulting from any ideas, methods, instructions or products referred to in the content.